Spectroscopic ellipsometric investigation of graphene and thin carbon films from the point of view of depolarization effects

Z. Pápa,[1,a)] J. Csontos,[1] T. Smausz,[1,2] Z. Toth,[3] and J. Budai[1]

[1]*Department of Optics and Quantum Electronics, University of Szeged, Szeged, H-6720, Hungary*

[2]*MTA-SZTE Research Group on Photoacoustic Spectroscopy, University of Szeged, Szeged, H-6720, Hungary*

[3]*Department of Oral Biology and Experimental Dental Research, University of Szeged, Szeged, H-6720, Hungary*

A spectroscopic ellipsometric study of single-, double- and five-layer graphene transferred to thick SiO_2 support layers is presented. Depolarization measurements showed significant peaks. To understand the nature of this depolarization, a sample series consisting of SiO_2 support layers of different thicknesses covered with thin pulsed laser deposited carbon layers is also studied. Our investigations show that depolarization originates both from the measurement conditions and from the sample properties, and becomes significant due to the presence of the support layer. Our findings reveal that the observable depolarization peaks diminish with the increase of absorption and thickness of the layer covering the support layer. Since the support layer is generally used to increase the sensitivity of ellipsometry based on the interference enhancement method, we study the influence of depolarization on the results of ellipsometric evaluation. It is shown that neglecting depolarization during the analysis can cause significant inaccuracy in the deduced thickness and optical properties of graphene. This difference decreases with increasing layer number, i.e. with increasing graphene thickness. This effect is also shown for thicker test carbon layer series.

[a)] Corresponding author. Electronic mail: zpapa@titan.physx.u-szeged.hu.

I. INTRODUCTION

Exploring the optical properties of graphene has been the goal of an intensive research during the last few years. Spectroscopic ellipsometry (SE) is a contact-free and widely applied tool of this research. Ellipsometry is not only capable of investigating the optical response of 2D materials; but it has already been used to discover that the deduced refractive index of graphene depends on several sample properties. Among them the most important ones are the production technique used (including exfoliation of graphene flakes [1-3], epitaxy on SiC [4-6], and chemical vapor deposition (CVD) on transition metals like copper and nickel [7-10]); the type of the substrates; and in the case of transferred graphene, the possible presence of an interlayer between the substrate and graphene [8,10]. In the following, it will be shown that besides these parameters the measurement circumstances may affect the ellipsometric evaluation itself, also influencing the deduced optical properties of graphene and other 2D materials.

Generally, ellipsometry is applied to determine the optical properties and thicknesses of thin films by measuring the polarization change of a probe light upon reflection on the sample, and by modeling and fitting the measured ellipsometric data. The simultaneous determination of film thickness and optical properties for thin films below ~ 10 nm is challenging, since in such cases these data are rather correlated which deteriorates the sensitivity of ellipsometric measurements. It is more complicated if the film is absorbing since beside the refractive index (n) the extinction coefficient (k) values need to be deduced as well. These two layer properties, namely that they are ultrathin and absorbing, are certainly true for most 2D materials, therefore in the case of their ellipsometric investigation the sensitivity of ellipsometry has to be increased. For this purpose, the interference enhancement method is applied widespread [11-13]. This method is based on the application of a thick, transparent, well-defined support layer. The presence of this thick dielectric layer below the absorbing layer under study increases the change in the optical path length, and

provides new information from measurements at multiple incidence angles [14,15]. A typical sample for this method is a thin (< 50 nm) absorbing film (the film under study) deposited on a thick (> 100 nm) transparent layer (the support layer) on a silicon substrate [14]. The absorbing layer must be thin enough to allow a significant fraction of the illuminating light to leave the sample after i) traversing the absorbing and transparent layer, ii) being reflected from the substrate, and iii) traversing again the two overlayers. When this condition is fulfilled, interference oscillations appear in the ellipsometric data, and the sensitivity of ellipsometry is enhanced to both film thickness and optical constants of the absorbing layer.

Unfortunately, the sensitivity of ellipsometry decreases in cases when the reflected beam contains multiple polarization states, i.e. when the measurement conditions depolarize the probe beam. For example, depolarization certainly appears when measurements are performed with focused beams, which is necessary for samples that can be considered homogeneous only in small area (e. g. graphene and other 2D materials often exist in the form of flakes [1,2,16,17]). There are other possible sources of depolarization which can occur in the case of parallel beam measurements as well, and which may affect the results of the ellipsometric evaluation, like the finite bandwidth of the spectrograph [18, 19] and the inhomogeneity of film thickness. Most of the depolarization sources can be handled during the evaluation [20-23]. The description and handling of these sources are in the focus of intense research, meaning not only the development of new mathematical formulae [24], but also new measurement techniques [25]. However, up to our knowledge the effect of depolarization has not been investigated in case of interference enhancement method applied to ultrathin films like graphene.

Therefore, in this study, we have examined the optical properties of graphene samples of different layer numbers and investigated the sensitivity of ellipsometry if the interference

enhancement method is applied in depolarizing circumstances. To gain a deeper understanding of the depolarization observed in the case of graphene samples, a test sample series was produced and evaluated, which consists of thermally grown SiO_2 layers with carbon coatings of different thicknesses. It will be shown that in certain thickness ranges depolarization can have a significant effect on the deduced optical properties of the investigated layer.

II. EXPERIMENTAL

We investigated different commercially available graphene samples by spectroscopic ellipsometry. Three CVD graphene samples from ACS Material, LLC - single-, 2- and 5-layer graphene transferred to 300 nm thick SiO_2 layer - were studied. To confirm the layer numbers of the graphene samples Raman spectroscopy was employed. Raman spectra were recorded by a Thermo Scientific DXR Raman microscope. The excitation wavelength was 532 nm; spectra were recorded in the 50-1860 cm^{-1} range with ~3 cm^{-1} resolution.

Graphene sheets are usually transferred to silicon dioxide for easier visualization of their coverage, since a certain thickness of SiO_2 drastically enhances the visibility of graphene [26]. Silicon dioxide is often used as support layer in interference enhancement method as well [2, 11-14]. In this study, to understand the behavior of the graphene samples graphite-like carbon layers on thick SiO_2 were also studied. For this purpose, we created a matrix of carbon-coated SiO_2 samples with five different SiO_2 thicknesses and six different carbon thicknesses. The five SiO_2 layers in the thickness range of 30-660 nm were grown thermally by heating silicon wafers at 1000 °C in air ambient applying different annealing times. These layers were later used as transparent support layers for the thin carbon layers, which were produced by pulsed laser deposition (PLD). In the PLD setup, a glassy carbon target was used, which was ablated by a KrF excimer laser in 1 Pa argon background. The SiO_2 layers were coated with carbon layers by applying 1000 and 20 laser

pulses. The lateral thickness distributions of the carbon thin films belonging to the same pulse numbers were the same, since the spatial distribution of the laser plasma was permanent at each deposition process. The two different laser pulse numbers and the thickness distributions allowed selecting carbon film domains with 6 different nominal thickness values in the range of 8 to 60 nm at each SiO_2 thickness value. A more detailed description of the SiO_2 and carbon layers of the 5×6=30 samples is given later..

A rotating compensator spectroscopic ellipsometer (Woollam M-2000F) was used to measure the Ψ, Δ and depolarization values in the 275-1000 nm (1.24-4.5 eV) range at 462 photon energies. Depolarization measurements were performed assuming isotropic behavior of the samples, allowing the determination of the M_{12} *(N)*, M_{33} *(C)* and M_{34} *(S)* Mueller-matrix elements without the measurement of the full Mueller-matrix. These independent non-zero elements can be calculated from Ψ and Δ as follows [27]:

$$N=\cos 2\Psi \tag{1}$$

$$C=\sin 2\Psi \cos\Delta \tag{2}$$

$$S=\sin 2\Psi \sin\Delta \tag{3}$$

The sum-square of these elements is equal to one only if the sample is non-depolarizing, so it corresponds to the degree of polarization, therefore depolarization is defined by [28]:

$$D = 1 - (N^2 + C^2 + S^2) \tag{4}$$

Measurements were carried out with parallel and focused light beams (the minor axis of the focused beam is 150 μm) at 60°, 65° and 70° angles of incidence (AOI). When using focusing optics the shift of the incidence angle was measured to be 0.2° on a standard silicon wafer and later fixed during the analysis. Four measurements were performed on all graphene samples which were simultaneously analyzed. When performing measurements on our PLD carbon films, the same lateral position was chosen on each sample to ensure the measurement of film domains of similar thicknesses. Evaluation of the spectra was carried out with WVASE32 software. For evaluation, the

multisample method was used [15], which allows the simultaneous analysis of data measured on different samples with the same set of optical constants to describe all films. For more details of the modeling see the Results and discussion section. The quality of fitting was classified using the mean squared error (MSE) [29] values defined as follows:

$$MSE = \sqrt{\frac{1}{2N-L}\sum_{i=1}^{N}\left(\left(\frac{\Psi_i^c - \Psi_i^m}{\sigma_i^{\Psi}}\right)^2 + \left(\frac{\Delta_i^c - \Delta_i^m}{\sigma_i^{\Delta}}\right)^2\right)}, \quad (5)$$

where L is the number of fitting parameters and N denotes the number of measurement points. In the case of Ψ and Δ, the c and m superscripts denote the calculated and measured values, respectively. σ^{Ψ} and σ^{Δ} are standard deviations related to Ψ and Δ data. The reported errors were calculated using 95% confidence level in all cases.

III. RESULTS AND DISCUSSION

When performing measurements on the graphene samples with focused beam, notable depolarization was observed on each sample. Figure 1 a), b) and c) show the Ψ, $\langle n \rangle$ and the depolarization curves belonging to the single-layer graphene sample.

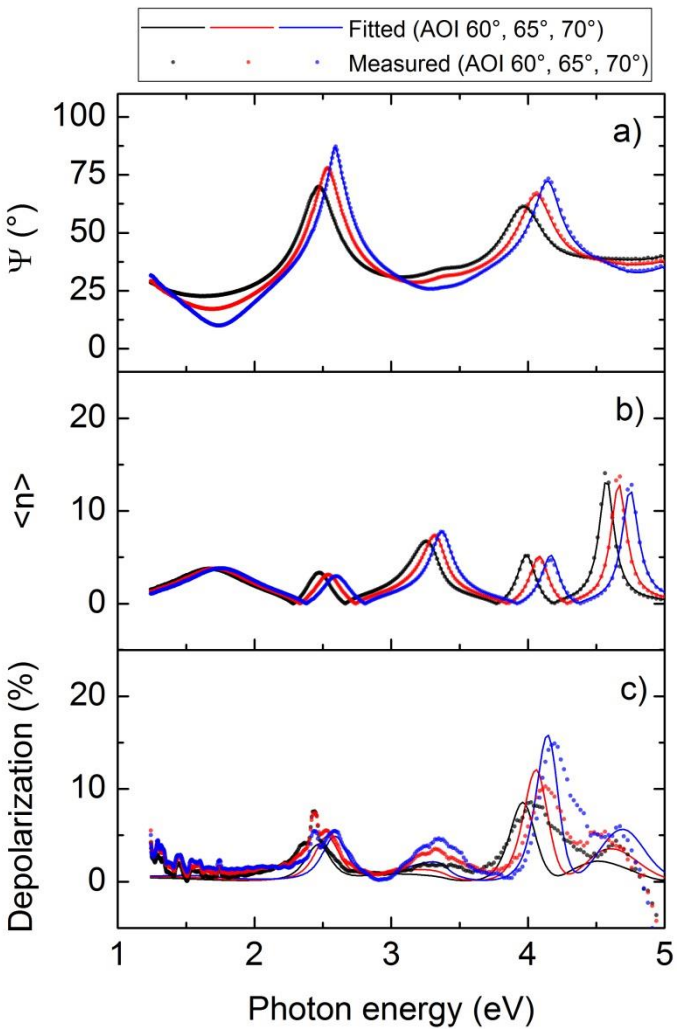

FIG.1. a) Ψ curves, b) <*n*> curves and c) depolarization spectra of the single layer graphene sample at 60, 65 and 70°AOI. The fitted curves using the method described in Section C are also presented with solid lines.

It can be seen from Figure 1 that the positions of the main depolarization peaks correlate with the interference oscillations of the Ψ spectra. This coincidence is more prominent in the case of <*n*> curves. Since the source of these oscillations is the interference between light reflected from the top and bottom of the support layer, the shape and position of the oscillations depend mainly on - beside the measurement conditions - the thickness and optical properties of the support layer. Therefore the correlation of the depolarization peaks with the peaks of the ellipsometric spectra indicates that though the depolarization sources can be sample or measurement related the

properties of the structures are mainly present due to the support layer and not graphene itself. This is also supported by the observation of Abdallah et al [18], who presented similar depolarization curves in the case of $Ni_{1-x}Pt_x$ thin films deposited onto 200 nm thick SiO_2. Thus in the followings, before proceeding to the determination of the optical properties of graphene, it will be shown and discussed under which circumstances depolarization appears when thermally grown silicon dioxide is used as support layer.

A. Depolarization of SiO_2 layers and its possible sources

The depolarization curves of thermally grown SiO_2 support layers are presented in Figure 2. To investigate the possible depolarization sources measurements were carried out both with parallel and focused beams (Figure 2 a) and b), respectively). Notable depolarization was obtained in both cases, and the depolarization spectra showed similar periodic structure: more peaks are present in the case of thicker layers, and the peak positions for the same layer thickness are the same with both beam types.

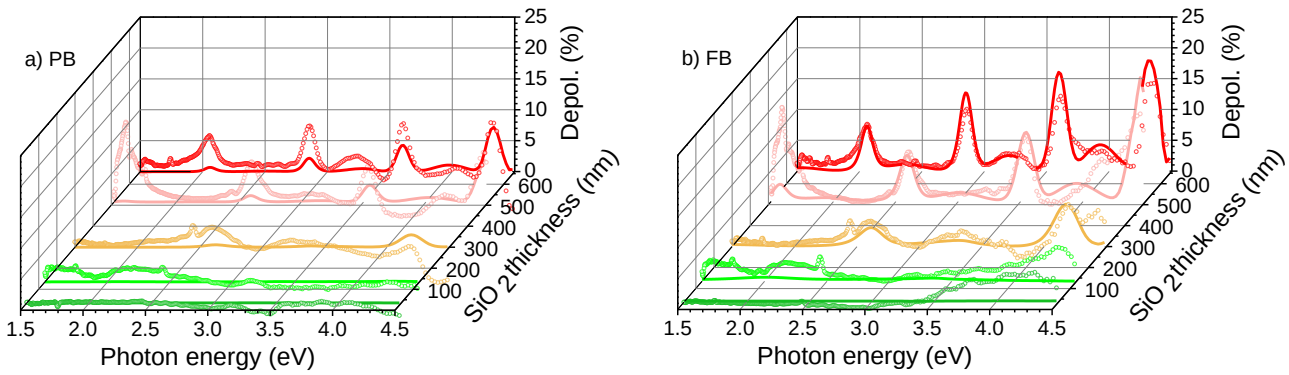

FIG.2. Depolarization measured on thermally grown SiO_2 layers with a) parallel (PB) and b) focused beam (FB) at 65° angle of incidence. The open circles present the measured data, while the solid lines correspond to the calculated depolarization 4 nm bandwidth of spectrograph was

assumed with a) a slight inhomogeneity in the sample properties in the case of PB measurements, and b) 3°angular spread in the case of FB measurements.

To understand the nature of these depolarization curves, it should be taken into account that there are depolarization types which are inherently present during measurements. The finite bandwidth of the spectrograph and the angular spread of the beam always result in the presence of different polarization states [20], although the actual value of the measured depolarization also depends on the features of the sample under study. Sample related depolarization sources, namely inhomogeneous layer properties, surface scattering, or incoherent reflection of the probing beam from the backside of a transparent substrate can also be present [20]. In the case of our samples, the latter two effects can be excluded since the surfaces of the samples were smooth and the Si substrate is absorbing in the investigated spectral range. However, because of the finite bandwidth, the angular spread of the beam and the inhomogeneous layer properties, quasi-depolarization can occur. These depolarization types can be handled during the evaluation by taking into account that different portions of the light reaching the detector have different polarization states. During the analysis of our samples it was supposed that these parts add up incoherently. In this case the effect of quasi-depolarization can be quantified by averaging the Mueller-matrices corresponding to the different parts [28].

Discussing first the parallel beam measurements, it can be stated that angular spread is not relevant; therefore the possible quasi-depolarization sources are the finite bandwidth of the spectrograph and the inhomogeneity in layer properties. The bandwidth of our instrument was found to be 4 nm [30], which - as a standalone depolarization source - is not able to explain the measured depolarization curves. It is not only the absolute values of the measured depolarization curves that cannot be reproduced, but their shapes are different as well. The height ratio of the measured neighboring peaks is almost constant (see Figure 2 a)), while the height of the peaks in

the calculated spectra increases much faster towards the UV range, also shown by [18]. Therefore the measured peaks cannot be reproduced with further increment of the bandwidth value indicating that at least one other depolarization source is present.

The observed structure of the depolarization spectra can be described with additional layer thickness inhomogeneity. To investigate this possibility, thickness maps were recorded from each SiO_2 layer. SE measurements using focusing optics were performed at 9 different points on an area of 5×5 mm^2 size. The thickness map of the SiO_2 layer with 515 nm nominal thickness is presented in Figure 3.

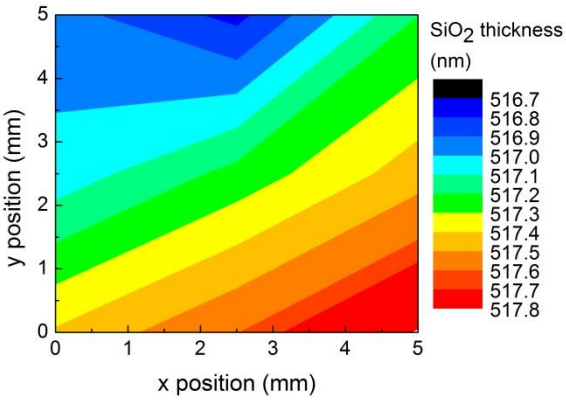

FIG.3. Thickness map of the SiO_2 layer with nominal thickness value of 515 nm.

According to the thickness maps, the layer thicknesses vary on average 2 nm along a 5 mm distance. Since the minor axis of the elliptical probing spot is in the range of a few hundred microns in the case of focusing probes and 1-2 millimeters in the case of parallel beam, this layer thickness variation cannot explain the measured depolarization. To reproduce the observed depolarization shown in Figure 2 a), the thickness variation within the spot of the parallel beam should be almost an order of magnitude larger than the actual thickness inhomogeneity of the layers.

Our simulation showed that a minor inhomogeneity in the optical properties of the SiO_2 layer can cause such depolarization effect. A patterned layer of which 3% has slightly different refractive index (dn~0.03) increases the depolarization enough to reproduce the measured depolarization

curves (see Fig. 2). Since the exact description of this refractive index variation is beyond the scope of this article, as a next step, it was investigated whether these effects can be eliminated if the ellipsometric data is collected from a much smaller sample domain using focusing optics.

If the measurements are performed with focusing probes, angular spread of the probing beam can cause depolarization since the different rays of the beam have slightly different incidence angles and they are travelling different optical path lengths in the transparent support layer. The extent of this kind of depolarization can be precisely calculated after measuring the divergence of the beam. The beam divergence of our instrument is measured to be 3°, so angular spread of the beam was taken into account with this value during fitting, along with the bandwidth which was fixed at 4 nm. Figure 2 b) shows that these two depolarization sources describe well the measured curves indicating that the effect of other possible depolarization sources can be neglected. This was further tested by allowing the fitting algorithm to adjust the thickness inhomogeneity parameter the values of which were around ~0.1 percent in all cases after fitting. According to these observations, the subsequent results were achieved by the evaluation of the focused beam measurements.

B. Diminution of depolarization of SiO_2 covered with different carbon layers

As it was shown previously, depolarization occurs when only the support layer is present. In the following, it will be investigated how this depolarization is altered if the support layer is coated with a thin absorbing layer. To examine the effect of film thickness, measurements were performed on the 30 sample domains belonging to different carbon and SiO_2 thickness values. To enable a simple comparison of the 30 depolarization curves, spectral average of depolarization values were calculated and plotted as function of SiO_2 and carbon layer thickness in Figure 4 a). The average values of depolarization presented in Figure 4 a) are smaller than 4%, which might seem to be negligible. However, when considering the whole spectra, spectral regions are present where maximum depolarization values can far exceed the average value. As an example, the measured

depolarization spectra of coated SiO_2 layers are presented Figure 4 b) and their average depolarization is denoted with dots also in the 3D surface plot of Figure 4 a). These figures show that as carbon layer thickness increases, the amplitude of the oscillations in the depolarization spectra decreases, and finally they become comparable with the noise level (Figure 4 b)). Furthermore, depolarization also becomes less significant when the SiO_2 layer gets thinner. From the point of view of ultrathin absorbing layers, this suggests that when applying thermally grown SiO_2 layers as support layer, the presence of the unknown 2D layer cannot significantly diminish the depolarization. Therefore in the following, we will investigate how the evaluation of ellipsometric data recorded on the graphene samples is altered when depolarization is neglected or handled.

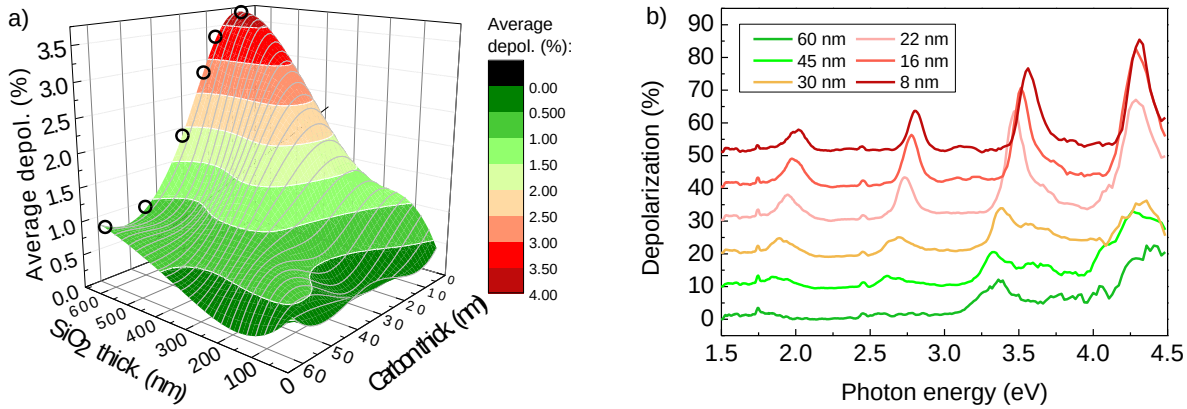

FIG.4.a) Average depolarization of the investigated samples as a function of SiO_2 thickness and carbon thickness. Black circles indicate the average depolarization of 660 nm SiO_2 samples covered with carbon layers of different thicknesses, the depolarization spectra of which are presented in Figure 4 b). For better visibility, each spectrum of Fig. 4 b) is shifted with a value of 10%. Results of focused beam measurements are presented.

C. Evaluation of graphene samples

As a first step of the ellipsometric evaluation, it was checked how the optical properties of the SiO_2 layers depend on their thickness, since the thickness of the investigated SiO_2 films vary in a wide range. In accordance with [31,32], it was found that the optical properties of the thinnest SiO_2 layer (35 nm) slightly differ from those determined for the thicker ones. For modeling the optical properties of SiO_2, Sellmeier-dispersion was used, the parameters of which were fixed later during the evaluation of the graphene and carbon coated samples.

Since the measurements of the graphene samples were carried out using focused beams, two approaches were used during evaluation: the first approach neglected depolarization while the second one handled it by taking into account the 4 nm bandwidth and the 3° angular spread. Each sample was measured at four different points and the datasets belonging to the same sample were evaluated jointly within one multisample environment using the following layer structure: a silicon substrate (optical functions from [31]), a silicon dioxide layer with different thickness values (optical properties described with Sellmeier-dispersion) and a graphene layer. This evaluation enabled us to couple the thickness and the optical properties of graphene, supposing that in the different measurement positions the graphene has the same optical behavior and the same thickness. The joint thickness and dispersion of the graphene could be varied slightly from sample to sample and the thickness of the underlying SiO_2 layer was allowed to be fine-tuned at each measurement position. To describe the optical properties of graphene a general oscillator layer was built up from a Drude-, and two Lorentzian-type oscillators. During evaluation, the anisotropy of graphene was not taken into account, since in the case of uniaxial systems having the optical axis perpendicular to the sample surface and having sub-nm thickness, ellipsometry is not sensitive to the out of plane polarization [5,9]. Table I contains the resulting film thicknesses along with the corresponding MSE values.

TABLE I. Film thicknesses of graphene layers obtained from multisample modeling. The values originating from both approaches, handling and neglecting depolarization are presented.

Graphene layer number	Thickness with depolarization (nm)	MSE with depolarization	Thickness without depolarization (nm)	MSE without depolarization
1	0.313	14.19	0.662	14.83
2	0.643	7.14	0.911	7.42
5	1.657	14.49	1.862	15.83

According to Table I the resulting film thickness values are rather different for the two approaches; therefore Raman spectroscopic measurements were carried out in order to verify the nominal layer numbers of the graphene samples. For the analysis of Raman spectra the position of the *G* peak located around 1580 cm^{-1} (Figure 5) was investigated, since the *G* peak shifts linearly as a function of the layer number [33,34]. The measured peak positions (1588.4 cm^{-1}, 1585.6 cm^{-1}, 1583.6 cm^{-1} for the single, double and five layer graphene) support the nominal layer numbers, which are furthermore in good agreement with the results of the approach that handled depolarization. The stability of the ellipsometric fitting was also checked: minimized MSE values were calculated at different fixed thickness values around the ones determined by the minimization algorithm (insets of Figure 5). According to the insets the thickness values have a clear minimum around 0.32 nm, 0.65 nm and 1.66 nm supporting that the chosen optical model is reasonable.

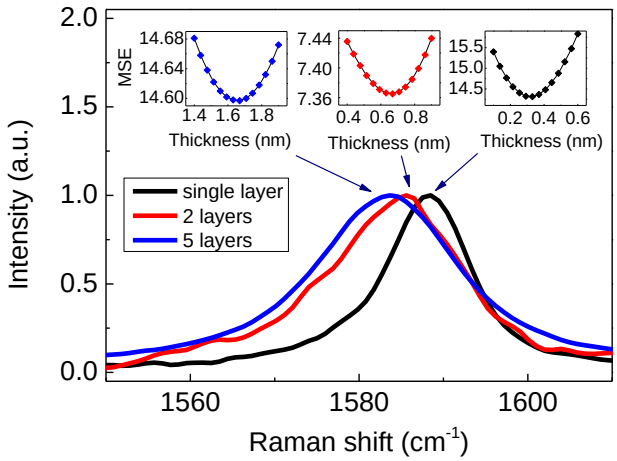

FIG.5. *G* peak of the Raman spectra measured on the three different samples. Results of the thickness uniqueness fits of the ellipsometric analysis approach handling depolarization are shown in the insets.

Optical functions resulting from the analysis are presented in Figure 6. Dashed lines correspond to the deduced optical functions in the case of the approach neglecting depolarization, while the solid lines show the optical functions resulting from the approach handling depolarization. The uncertainty of the optical functions (10%) indicated with gray regions around the curves was estimated from the uncertainty of the fitting parameters provided by the software.

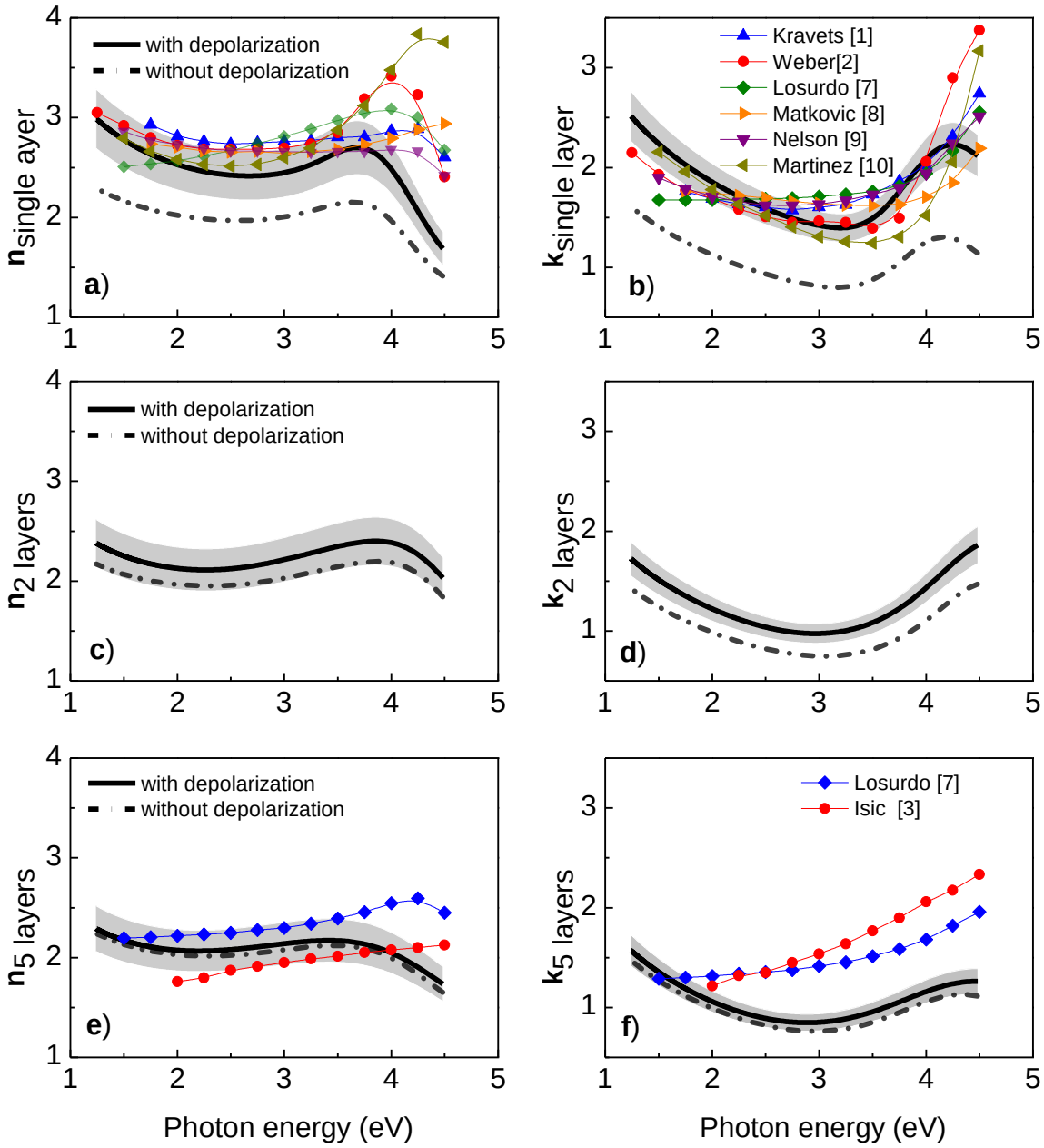

FIG.6. a)-e) Refractive index and extinction coefficient of the different graphene samples (a) and b): single layer, c) and d): 2-layers, e) and f): 5-layers) deduced from the analysis of SE data handling (continuous line) and neglecting (dashed line) depolarization sources. In the case of single-layer graphene and 5 layers graphene the results of References [1-3,7-10] and References [7,3] are also presented.

When comparing the n and k curves obtained with the two approaches, the largest difference can be observed in the case of the thinnest sample. As the graphene layer number increases the two curves almost overlap indicating that the effect gets less significant. The difference between the curves is almost constant, namely in the refractive index the average difference is 0.53 for the single layer, 0.18 for the 2-layer and less than 0.1 for the 5-layer sample, while the average difference in the extinction coefficient is 0.77, 0.27 and 0.1, respectively. As shown above, beside the optical properties the resulting thickness values also differ for the two approaches (Table I). When the 3° angular spread and 4 nm bandwidth were neglected, the fitted graphene thicknesses became larger with ~ 0.3 nm in all cases. This value is in the range of the nominal thickness of single-layer graphene, suggesting that the large deviation in the deduced optical properties of single-layer graphene is due to thickness deviations comparable to film thickness. When the film thickness exceeds this deviation value the optical properties are less altered by the uncertainties in the fitted film thicknesses caused by neglecting depolarization. This also suggests that the large deviation can be avoided if the thickness is known from an independent measurement (e. g. atomic force microscopy). However, as shown above, ellipsometry is also capable of providing the thickness of such ultrathin layers, if the measurement conditions are known and taken into account.

It has to be noted that if depolarization was neglected we would get almost the same n-k values for graphene samples of different layer number. In that case all optical curves would lay between 1.4 and 2.3 for n, and between 0.7 and 1.6 for k. However, when depolarization is taken into account the deduced optical properties of single layer graphene are higher, namely n changes between 1.7 and 3 while k changes between 1.5 and 2.5. These values are in accordance with data from literature as shown in Fig 6 a) and b). The results of the approach handling depolarization show that with increasing layer number the optical functions shift down. The average decrease for 2-layers graphene compared to single layer is 0.4 for n and 0.6 for k, while in case of 5-layers these

values are 0.5 and 0.8, respectively. As the layer number increase it could be expected that the deduced optical properties resemble that of graphite [35], however, the observed decrease in n and k shows an opposite tendency. Similar behavior of few-layer graphene samples was observed by References [3,7].

D. Evaluation of the PLD carbon layer samples

Our observations show that film thickness values and optical properties resulting from the two approaches differ significantly. However, it was also observed that the deviation decreases with increasing film thickness. Thus it is expected that the influence of depolarization will vanish in the case of conventional thin films of a few-tens of nanometers thickness, which are typical subject of interference enhancement method. To support experimentally this expectation, ellipsometric data recorded on PLD carbon thin film series were also evaluated with the two approaches neglecting and handling depolarization.

During the ellipsometric modeling of the carbon thin films, they were handled as isotropic samples, since the rather high D-peak in their Raman spectra (for the Raman spectra of a typical film see Fig 7 a)) indicated that they do not have the perfect crystalline nature of graphite. The spectra showed that their structure is closer to that of microcrystalline graphite exhibiting crystalline domains of different orientations, averaging out any anisotropy [36,37]. Furthermore, it was expected that layers of the same nominal thickness have the same optical behavior. Therefore, to reduce uncertainty, a multisample model was built for each nominal carbon thickness with different SiO_2 thicknesses. The six multisample environments are represented by columns in Table II, where the results of the fittings are summarized. It is well-known that the properties of PLD thin layers show lateral dependency [38], so different dispersion characteristics were allowed at different nominal carbon thickness values; however, within one multisample environment – handling carbon film domains of the same nominal thickness – the carbon layer optical properties were coupled. To

describe the optical behavior of carbon thin films, a general oscillator layer was applied containing the same oscillator types as in the case of graphene. The carbon and SiO_2 layer thicknesses were allowed to change slightly during fitting. It was checked after each fitting procedure that the SiO_2 thicknesses remained close to the value which was measured before deposition.

TABLE II. Film thicknesses of carbon layers obtained from multisample modeling. Each column belongs to one multisample environment. The presented values correspond to the approach handling depolarization.

Carbon nominal thick. (nm) / SiO_2 nom. thick. (nm)	60	45	30	22	16	8
35	53.13	43.36	32.88	21.37	18.03	11.25
135	58.43	43.14	28.44	20.76	15.20	6.28
300	59.72	44.72	30.52	24.50	10.93	6.45
515	64.15	47.10	31.54	21.78	16.28	6.82
659	62.52	46.42	36.39	20.90	10.64	9.39
MSE	17.57	28.10	23.76	25.74	20.11	21.2

The MSE values presented in Table II support that the fitting results are appropriate. We have to note, that the MSE values of the two approaches remained almost the same for the thicker carbon layers, but an average of 5% improvement was observed in the MSE values for carbon layers below 10 nm if the depolarization parameters were introduced.

A resulting optical function of a typical PLD carbon layer is shown in Figure 7 b). The lower refractive index and extinction coefficient of PLD carbon layers compared to ordinary optical properties of graphite [35] can be explained by the structure of the layer, which is strongly influenced by the deposition conditions. Since deposition was performed in 1 Pa argon background, the layers are supposed to be less compact [39], giving rise to the observed decrease in the optical functions.

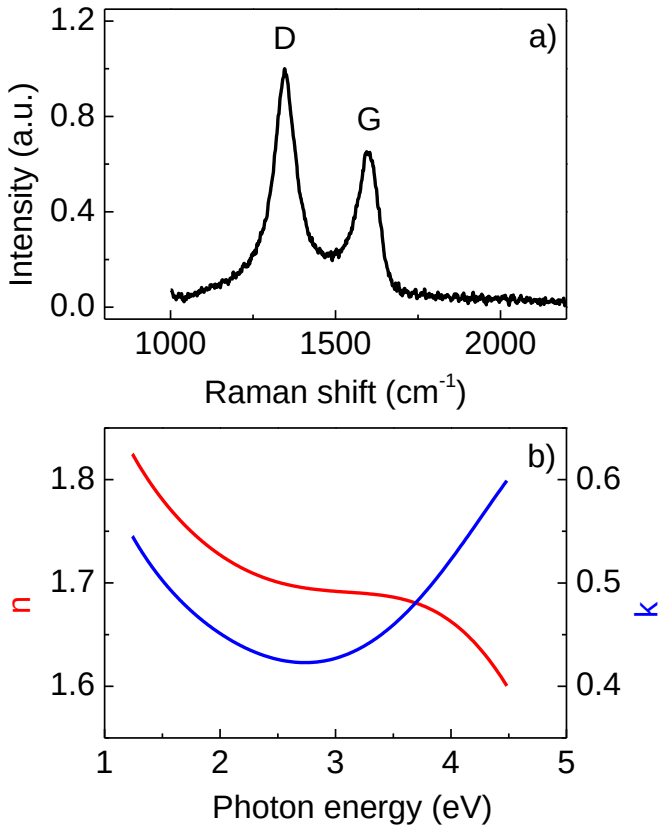

FIG.7. a) Raman spectrum of a typical PLD carbon layer and b) the corresponding average *n* and *k* values.

The graphitic character of the PLD samples enables us to compare the depolarization sensitivity of the deduced optical properties of PLD-grown carbon thin films to that of graphene. In order to present this sensitivity in different carbon thickness ranges, the difference between the *n* and *k* values resulting from the approaches neglecting and handling depolarization sources were

calculated at each point of the spectrum. The differences were averaged and plotted as a function of carbon layer thickness in Figure 8 along with the differences observed for graphene.

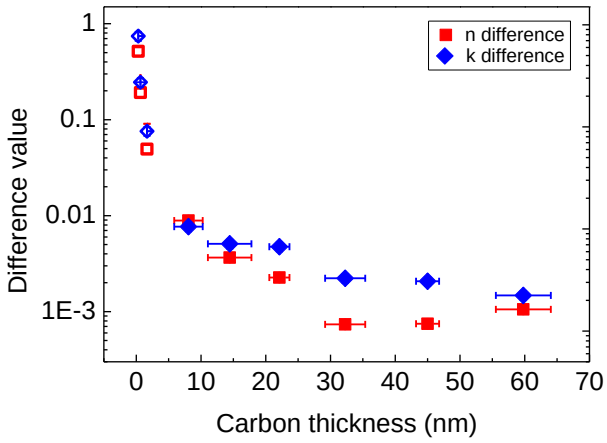

FIG.8. Differences between the average *n* and *k* values of the graphene (open symbols) and carbon layers (solid symbols) evaluated with and without depolarization.

As it can be seen from Figure 8 if the thickness of the carbon layer increases above a certain value, the difference of *n* and *k* values is no more relevant. When carbon thickness decreases, i.e. when the depolarization becomes more significant, the difference values increase. These results show that depolarization cannot be neglected when the absorbing layer under study is thinner than a threshold thickness. This threshold value in the case of our PLD grown carbon layers is around 30 nm. According to our simulation results (not presented) the threshold thickness is smaller in the case of materials with larger extinction. A simple explanation is that if the refractive index and the extinction coefficient of the layer get higher, a smaller amount of light is reflected from the substrate-SiO_2 interface. Thus a smaller amount of radiation traveling through the SiO_2 layer can be detected. Therefore the apparent enhancement of the depolarization caused by the interference of the light reflected from the top and bottom of the layer has a smaller contribution to the spectra. This means, for graphite as an example, the depolarization related differences of the deduced optical

parameters are only significant in the case of layers having thicknesses less than 10 nm. Since graphene has a similar extinction to the ordinary dielectric function of graphite [35] and its thickness is always smaller than this threshold value, depolarization has a large influence on the deduced optical properties of graphene, in accordance with the results presented in Section C and Figure 8.

IV. CONCLUSIONS

In this work, we have determined the optical properties of single-, 2- and 5-layer graphene using the interference enhancement method, and we have studied the effects of depolarization on the deduced optical data. We have shown that if depolarization sources are present, increased depolarization will be observed due to the presence of the support layer, which is necessary for the interference enhancement method. According to our findings, neglecting depolarization results in a thickness deviation commensurable with the thickness of single-layer graphene causing significant error in the optical properties. For thin carbon film series it was presented that this effect decreases if the film thickness or the absorption of the film gets larger, as also predicted by the diminution of the depolarization. This decrease in the influence of depolarization was also revealed for graphene samples of different layer numbers. Our results indicate that it is very important to consider depolarization when applying interference enhancement method for ellipsometric analysis of ultrathin 2D materials.

ACKNOWLEDGMENTS

The authors are thankful to the Laser Ablation Group of University of Szeged for the use of the ecximer laser and for providing the graphene samples.

REFERENCES

[1] V. G. Kravets, A. N. Grigorenko, R. R. Nair, P. Blake, S. Anissimova, K. S. Novoselov, and A. K. Geim, Spectroscopic ellipsometry of graphene and an exciton-shifted van Hove peak in absorption, Physical Review B 81 (2010) 155413 1-6.

[2] J. W. Weber, V. E. Calado, M. C. M. van de Sanden, Optical constants of graphene measured by spectroscopic ellipsometry, Applied Physics Letters 97 (2010) 091904 1-3.

[3] G. Isic, M. Jakovljevic, M. Filipovic, D. Jovanovic, B. Vasic, S. Lazovic et al, Spectroscopic ellipsometry of few-layer graphene, Journal of Nanophotonics 5 (2011) 051809 1-7.

[4] F. Nelson, A. Sandin, D. B. Dougherty, D. E. Aspnes, J. E. Rowe and A. C. Diebold, Optical and structural characterization of epitaxial graphene on vicinal 6H-SiC(0001)–Si by spectroscopic ellipsometry, Auger spectroscopy, and STM, Journal of Vacuum Science and Technology B 30 (2012) 04E106-101.

[5] V. Darakchieva, A. Boosalis, A. A. Zakharov, T. Hofmann, M. Schubert, T. E. Tiwald, T. Iakimov, R. Vasiliauskas, and R. Yakimova, Large-area microfocal spectroscopic ellipsometry mapping of thickness and electronic properties of epitaxial graphene on Si- and C-face of 3C-SiC(111), Applied Physics Letters 102 (2013) 213116 1-5.

[6] A. Boosalis, T. Hofmann, V. Darakchieva, R. Yakimova, and M. Schubert. Visible to vacuum ultraviolet dielectric functions of epitaxial graphene on 3C and 4H SiC polytypes determined by spectroscopic ellipsometry, Applied Physics Letters 101 (2012) 011912 1-4.

[7] M. Losurdo, M. M. Giangregorio, P. Capezzuto, and G. Bruno, Ellipsometry as a Real-Time Optical Tool for Monitoring and Understanding Graphene Growth on Metals, Journal Physical Chemistry C 115 (2011) 21804–21812.

[8] A. Matkovic, U. Ralevic, M. Chhikara, M. M. Jakovljevic, D. Jovanovic, G. Bratina and R. Gajic, Influence of transfer residue on the optical properties of chemical vapor deposited graphene

investigated through spectroscopic ellipsometry, Journal of Applied Physics 114 (2013) 093505 1-5.

[9] F. J. Nelson, V. K. Kamineni, T. Zhang, E. S. Comfort, J. U. Lee, and A. C. Diebold, Optical properties of large-area polycrystalline chemical vapor deposited graphene by spectroscopic ellipsometry, Applied Physics Letters 97 (2010) 253110 1-3.

[10] E. Ochoa-Martínez, M. Gabás, L. Barrutia, A. Pesquera, A. Centeno, S. Palanco et al, Determination of refractive index and extinction coefficient of standard production CVD-graphene, Nanoscale 7(4) (2015) 1491-500.

[11] M.T. Kief, G. Al-Jumaily, G.S. Mowry, Optical metrology for MR heads, IEEE Transactions on Magnetics 33 (5) (1997) 2926-2928.

[12] M. Campoy-Quiles, P.G. Etchegoin, D.D.C. Bradley. Exploring the potential of ellipsometry for the characterisation of electronic, optical, morphologic and thermodynamic properties of polyfluorene thin films, Synthetic Metals 155 (2005) 279-282.

[13] X. Liang, X. Xu, R. Zheng, Z. A. Lum, J. Qiu, Optical constant of CoFeB thin film measured with the interference enhancement method, Applied Optics 54 (2015) 1557-1563.

[14] W.A. McGahan, B. Johs, J.A. Woollam. Techniques for ellipsometric measurement of the thickness and optical constants of thin absorbing films, Thin Solid Films 234 (1993) 443-446.

[15] J. N. Hilfiker, N. Singh, T. Tiwald, D. Convey, S. M. Smith, J. H. Baker, H. G. Tompkins, Survey of methods to characterize thin absorbing films with Spectroscopic Ellipsometry Thin Solid Films 516 (2008) 7979-7989.

[16] R. Mas-Balleste, C. Gomez-Navarro, J. Gomez-Herrero and F. Zamora. 2D materials: to graphene and beyond, Nanoscale, 3 (2011) 20-30.

[17] G. R. Bhimanapati, Z. Lin, V. Meunier, Y. Jung, J. Cha, S. Das et al, Recent Advances in Two-Dimensional Materials beyond Graphene, ACS Nano 9 (12) (2015) 11509-11539.

[18] L. S. Abdallah, S. Zollner, C. Lavoie, A. Ozcan, M. Raymond, Compositional dependence of the optical conductivity of Ni1 − xPtx alloys (0 b x b 0.25) determined by spectroscopic ellipsometry, Thin Solid Films 571 (2014) 484-489.

[19] S. Zollner, T.-C. Lee, K. Noehring, A. Konkar, N. D. Theodore, W. M. Huang, D. Monk, T. Wetteroth, S. R. Wilson and J. N. Hilfiker, Thin-film metrology of silicon-on-insulator materials, Applied Physics Letters, 76 (2000) 46-48.

[20] H. Fujiwara. Spectroscopic Ellipsometry, Principles and Applications, John Wiley & Sons Inc., New York, 2007, p. 139-141.

[21] J.-T. Zettler, T. Trepk, L. Spanos, Y.-Z. Hu, W. Richter, High precision UV-visible-near IR Stokes vector spectroscopy, Thin Solid Films 234 (1993) 402-407.

[22] G. E. Jellison, Jr., J. W. McCamy, Sample depolarization effects from thin films of ZnS on GaAs as measured by spectroscopic ellipsometry, Applied Physics Letters 61 (1992) 512-514.

[23] Z. Pápa, J. Budai, I. Hanyecz, J. Csontos, Z. Toth. Depolarization correction method for ellipsometric measurements of large grain size zinc-oxide films, Thin Solid Films 571 (2014) 562-566.

[24] K. Hingerl, R. Ossikovski. General approach for modeling partial coherence in spectroscopic Mueller matrix polarimetry, Optics Letters 41 (2) (2016) 219-222.

[25] W. Li, C. Zhang, H. Jiang, X. Chen, and S. Liu, Depolarization artifacts in dual rotating-compensator Mueller matrix ellipsometry, Journal of Optics 18 (2016) 055701 1-7.

[26] P. Blake, E. W. Hill, A. H. Castro Neto, K. S. Novoselov, D. Jiang, R. Yang, T. J. Booth and A. K. Geim, Making graphene visible, Applied Physics Letters 91 (2007) 063124 1-3.

[27] H. G. Tompkins, E. A. Irene (Eds.), Handbook of Ellipsometry, William Andrew Inc., Springer, 2005, p. 453.

[28] B. Johs, J. A. Woollam, C. M. Herzinger, J. Hilfiker, R. Synowicki, and C. L. Bungay, Overview of Variable Angle Spectroscopic Ellipsometry (VASE), Part II: Advanced Applications Spie Proceedings CR72 (1999) 29-58.

[29] J. A. Woollam, B. Johs, C. M. Herzinger, J. Hilfiker, R. Synowicki, C. L. Bungay, Overview of variable-angle spectroscopic ellipsometry (VASE): I. Basic theory and typical applications Spie Proceedings CR72 (1999) 3-28.

[30] D. E. Morton, B. Johs and J. Hale, Optical Monitoring of Thin-films Using Spectroscopic Ellipsometry, Society of Vacuum Coaters 505/856-7188, 45th Annual Technical Conference Proceedings (2002) ISSN 0737-5921.

[31] C. M. Herzinger, B. Johs, W. A. McGahan, J. A. Woollam, W. Paulson, Ellipsometric determination of optical constants for silicon and thermally grown silicon dioxide via a multi-sample, multi-wavelength, multi-angle investigation, Journal of Applied Physics 83 (1998) 3323-3336.

[32] K. K. Christova, A. H. Manov, Mechanical stress and refractive index variation in dry SiO2, International Journal of Electronics 76 (5) (1994) 913-916.

[33] A. Gupta, G. Chen, P. Joshi, S. Tadigadapa, and P.C. Eklund, Raman Scattering from High-Frequency Phonons in Supported n-Graphene Layer Films, Nano Letters 6 (12) (2006) 2667–2673.

[34] H. Wang, Y. Wang, X. Cao, M. Feng and G. Lan, Vibrational properties of graphene and graphene layers, Journal of Raman Spectroscopy 40 (2009) 1791–1796.

[35] A. B. Djurisic, E. H. Li, Optical properties of graphite, Journal of Applied Physics 85 (10) (1999) 7404-7410.

[36] I. Pócsik, M. Hundhausen, M. Koós, L. Ley, Origin of the D peak in the Raman spectrum of microcrystalline graphite, Journal of Non-Crystalline Solids 227–230 (1998) 1083–1086.

[37] A. C. Ferrari, J. C. Meyer, V. Scardaci, C. Casiraghi, M. Lazzeri, F. Mauri, S. Piscanec, D. Jiang, K. S. Novoselov, S. Roth, and A. K. Geim, Raman Spectrum of Graphene and Graphene Layers, Physical Review Letters 97 (2006) 187401 1-4.

[38] A. Simon, T. Csákó, C. Jeynes, T. Szörényi, High lateral resolution 2D mapping of the B/C ratio in a boron carbide film formed by femtosecond pulsed laser deposition, Nuclear Instruments & Methods in Physics Research Section B - Beam Interactions with Materials and Atoms 249 (1-2) (2006) 454-457.

[39] J. Budai, Z. Tóth, A. Juhász, G. Szakács, E. Szilágyi, M. Veres and M. Koós, Reactive pulsed laser deposition of hydrogenated carbon thin films: The effect of hydrogen pressure, Journal of Applied Physics 100 (2006) 043501 1-9.